Observation of sound focusing and defocusing due to propagating nonlinear internal waves

J. Luo, M. Badiey, and E. A. Karjadi
College of Marine and Earth Studies, University of Delaware, Newark, Delaware 19716
luojing@udel.edu, badiey@udel.edu, karjadi@udel.edu

B. Katsnelson and A. Tskhoidze
Voronezh State University, Universitetskaya Sq. 1, Voronezh 394006, Russia
katz@phys.vsu.ru, tskhoidze@phys.vsu.ru

J. F. Lynch
Woods Hole Oceanographic Institution, Woods Hole, Massachusetts 02543
jlynch@whoi.edu

J. N. Moum
College of Oceanic & Atmospheric Sciences, Oregon State University, Corvallis, Oregon 97331-5503
moum@coas.oregonstate.edu

Abstract: Fluctuations of the low frequency sound field in the presence of an internal solitary wave packet during the Shallow Water '06 experiment are analyzed. Acoustic, environmental, and on-board ship radar image data were collected simultaneously before, during, and after a strong internal solitary wave packet passed through the acoustic track. Preliminary analysis of the acoustic wave temporal intensity fluctuations agrees with previously observed phenomena and the existing theory of the horizontal refraction mechanism, which causes focusing and defocusing when the acoustic track is nearly parallel to the front of the internal waves [J. Acoust. Soc. Am., **122**(2), pp. 747–760 (2007)].

PACS numbers: 43.30.Re, 43.30.Es, 43.30.Dr, 43.30.Bp [WC]
Date Received: March 15, 2008 **Date Accepted:** June 4, 2008

1. Introduction

In shallow water regions, nonlinear internal solitary waves (ISWs) create an anisotropic water column that affects acoustic wave propagation. In recent years, experimental and modeling efforts[1–3] have been conducted to quantify acoustic wave interaction with ISWs. These studies suggest that there are three different mechanisms that can explain the intensity variations in the presence of ISWs. The adiabatic regime corresponds to fluctuations of the sound field due to local variations of the water column (i.e., sound speed and/or depth) at the position of the source or the receiver. Next, propagation can be dominated by the mode coupling regime, where the interaction with the internal waves can cause energy transfer between different modes which in turn can result in fluctuations in the intensity. Finally, there is the horizontal refraction regime in which the distribution of the acoustic field in the horizontal plane can cause fluctuations in the measured field. The last two situations result in more significant signal intensity fluctuations than the first.[1–3] While the comparison of modeling results with data have previously shown the validity of this theory, a direct simultaneous measurement of the acoustic field and the ISW has not yet been reported to establish the transition among different mechanisms.

In our previous work, we separated propagation regimes depending on the angle between the ISW wave front and the direction of the acoustic track. In the Shallow Water '06 (SW06) measurements studied in this paper, we present a data set where the acoustic track angle is kept unchanged while the internal wave slowly transects the acoustic track for the source-receiver geometry. When the ISW train is starting to cover the receiver array only and does not

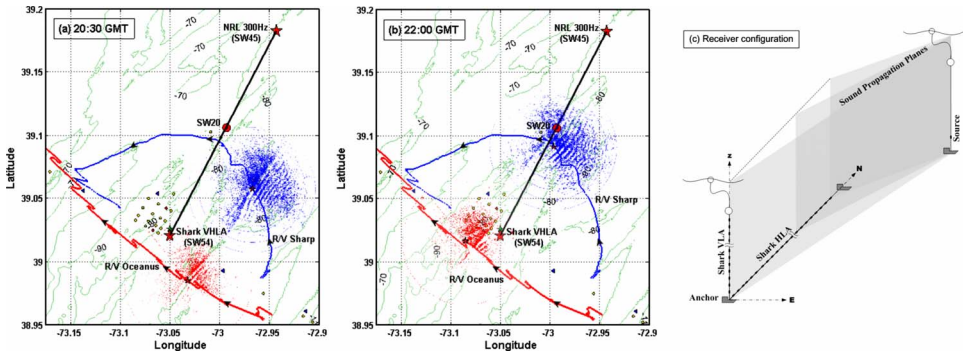

Fig. 1. (Color online) Map of the experiment location showing the positions of the acoustic source (NRL 300 Hz on SW45 mooring), the receiver array (Shark VHLA on SW54 mooring) and a midpoint thermistor array (SW20) together with the two research vessels (R/V SHARP and R/V OCEANUS) at two different geotimes. Times are (a) 20:30 GMT when the ISW has not reached the acoustic track, (b) 22:00:00 GMT when the ISW has occupied a large portion of the acoustic track including the receiver array. Ship tracks and radar images of R/V SHARP and R/V OCEANUS are shown. The configuration of the receiver Shark VLA and Shark HLA is shown in (c).

occupy all (or a significant part of) the acoustic track, we have the adiabatic regime. As the train moves and continues to cover the acoustic track, propagation changes to the horizontal refraction regime. Thus, we can isolate the transition between the two regimes.

The multi-institutional SW06 experiment was conducted on the New Jersey continental shelf from July to September 2006 at a location where internal wave activity has been observed and studied in the past.[4] In this paper, we focus on a particular internal wave event on August 17, 2006, for which a complete set of acoustic and environmental data were collected simultaneously. In addition, ISW surface signatures were captured continuously by the onboard radars of two research vessels prior to the arrival of, and during the passing of, the ISW packet over the acoustic track. The acoustic wave field variation is studied during this process. Other studies of the SW06 data in relation to three dimensional modeling are being conducted separately.[5]

2. Simultaneous acoustic and internal wave measurement

During SW06, both acoustic and environment data were collected simultaneously. In this paper we discuss the acoustic data from a particular acoustic source (NRL 300 Hz) on the mooring denoted SW45 (see Fig. 1). The source was located 72 m below the sea surface and 10.5 m above the sea floor at 39°10.957′ N, 72°56.575′ W, and transmitted 2.0489 second Linear Frequency Modulating (LFM) signals from 270 to 330 Hz every 4 s. Transmissions continued for 7.5 min and then repeated every half hour. A vertical and horizontal receiver array (the "Shark VHLA") on mooring SW54 was located at 39°01.252′ N, 73°02.983′ W, about 20.2 km south of the NRL source. The vertical part of the receiver array consisted of 16 hydrophones with 3.5 m spacing and was positioned in the water column from 13.5 to 77.75 m below the surface. The horizontal part of the array consisted of 32 hydrophones on the seafloor with spacing of 15 m, providing 478 m of horizontal aperture. The sampling rate of the array was 9765.625 Hz. The acoustic track and the locations of the source and receiver as well as the horizontal and vertical array configurations are shown in Fig. 1. The water depth along the acoustic track was about 80 m.

On August 17, 2006, at about 18:00 GMT, the R/V SHARP from the University of Delaware was located at 38°59.262′ N, 72°57.492′ W and the R/V OCEANUS from the Woods Hole Oceanographic Institution (WHOI) was located at 38°57.426′ N, 72°56.676′ W. Both platforms observed the origination of an ISW near the shelf break. This event was named Event 50 on R/V SHARP and ROSEY on R/V OCEANUS.

Figures 1(a) and 1(b) show the track of each vessel following this event from 18:00 GMT on August 17 to 02:00 GMT on August 18, 2006. The R/V SHARP's track was semicircu-

lar, centered at the WHOI vertical and horizontal line array (Shark VHLA) with the ship being positioned on the trough of the leading ISW front and moving with the advancing front. The R/V OCEANUS followed the same ISW packet from its initial location, while keeping a watch on the advancing wave front. Reversals in the track of R/V OCEANUS indicate where the wave packet was crossed, and during these periods, intensive profiling of temperature, density, turbulence, and sound velocity was conducted.

The two ships observed different parts of the ISW front, thus providing a large spatial coverage. The surface signatures of the ISW were digitally recorded by on-board ship radar images every 30 s. Combined radar images from the two vessels, each about 11.1 km in diameter, covered the receiver and about two thirds of the acoustic track. Mm. 1 shows a movie of the ships' radar images following the ISW during this event, from 18:00 GMT on 17 August to 02:00 GMT on 18 August, 2006. In this paper we discuss two situations: (1) when the ISW packet had not reached the acoustic track [time period T_{g1} (20:30 to 20:37 GMT)] and (2) when the ISW occupied most of the acoustic track [time period T_{g2} (22:00 to 22:07 GMT)]. The radar images from both vessels at 20:30 GMT and 22:00 GMT are shown in Figs. 1(a) and 1(b), respectively.

Mm. 1. Ships' radar movie during Event 50 (ROSEY) showing the movement of the internal wave. This is a file of type "gif" (10 MB).

At 20:30 GMT, the R/V SHARP radar showed ten distinct ISW fronts in a packet. At the same time, the R/V OCEANUS radar showed seven wave fronts with less curvature. The spacing between wave fronts in the packet varied from ~0.4 to 0.5 km for the leading wave fronts to ~0.2–0.3 km for the trailing waves. The ISW direction of propagation was about compass direction 300°.

At 22:00 GMT, most of the acoustic track including the receiver array was occupied by the ISW packet [see Fig. 1(b)]. The physical characteristics of the ISW packet during this time were similar to those at 20:30 GMT, except that its propagation direction was slightly changed. The R/V OCEANUS observed the ISW propagation direction close to the receiver to be about 310°. At the middle of the acoustic track (SW20), a propagation direction of 305° was observed on R/V SHARP. Note that the wave front was curved so there is a natural discrepancy between the propagation directions observed by the two ships. The angle between the ISW fronts and the acoustic track at midpoint was approximately 5° and varied along the acoustic track. The average speed of the ships following the ISW packet was about 1.8–2.0 knots, which was similar to the ISW propagation speed.

The SW45 mooring had 11 temperature sensors located at depth between 15 and 72 m and the SW54 mooring had 11 temperature sensors at 5–78.5 m. To get a spatial picture of the water temperature along the acoustic track, data from a third thermistor string (SW20) in the middle of the track was also used. This mooring had three temperature sensors between 14 and 40 m. All these sensors recorded temperature data every 30 s.

Figure 2 shows the temperature records at the acoustic source mooring SW45, the midpoint SW20, and the receiver mooring SW54 from 20:00 to 23:00 GMT on August 17, 2006. A solitary internal wave arrived at the receiver around 21:15 GMT, followed by a calm period of about 20 min. At around 21:40 GMT, the leading front of a strong ISW packet passed the receiver position. The ISW packet caused a sudden increase in the thermocline depth. At 22:20 GMT, the water temperature decreased slowly until 09:00 GMT the next day. The leading wave front was observed at SW20 at 22:02 and at SW45 at 22:15 GMT, respectively. If we assume the leading wave front is linear (it is not) and the wave speed is constant along the wave front, this suggests an angle of about 5° between the advancing front and the acoustic track.

Next, we show the acoustic signal arrival on the Shark VHLA during the two periods T_{g_1} and T_{g_2}. In order to show the intensity variations, we show the arrival of two different LFM pings on the array at geotimes separated by 102 s. In Fig. 3(a), the upper panel shows the acoustic signal on the VLA at 20:30:16 GMT while the lower panel shows the same signal arriving on the HLA. Figure 3(b) shows the same two arrays at 20:31:58 GMT. The parallel lines on the HLA data shown in the lower panels are due to the difference of arrival time on the HLA [see

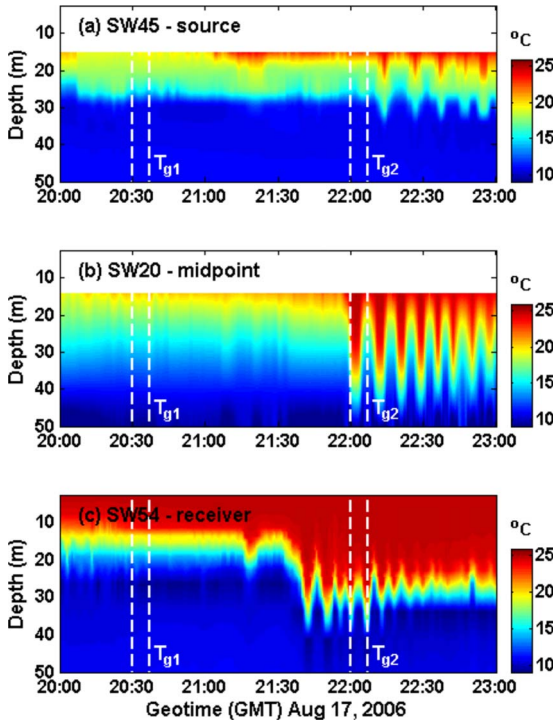

Fig. 2. (Color online) Temperature profiles measured at (a) the acoustic source, (b) the midpoint between the source and receiver, and (c) at the Shark WVHLA during internal wave Event 50, August 17, 2006 from 20:00 to 23:00 GMT. T_{g1}=20:30–20:37 GMT and T_{g2}=22:00–22:07 GMT.

array configuration in Fig. 1(c)]. The data on the VLA portion of the array shown in the upper panels best represent the modal arrivals. Note the similarity of the intensity values on both vertical and the horizontal array plots in Figs. 3(a) and 3(b), indicating the stability of the arriv-

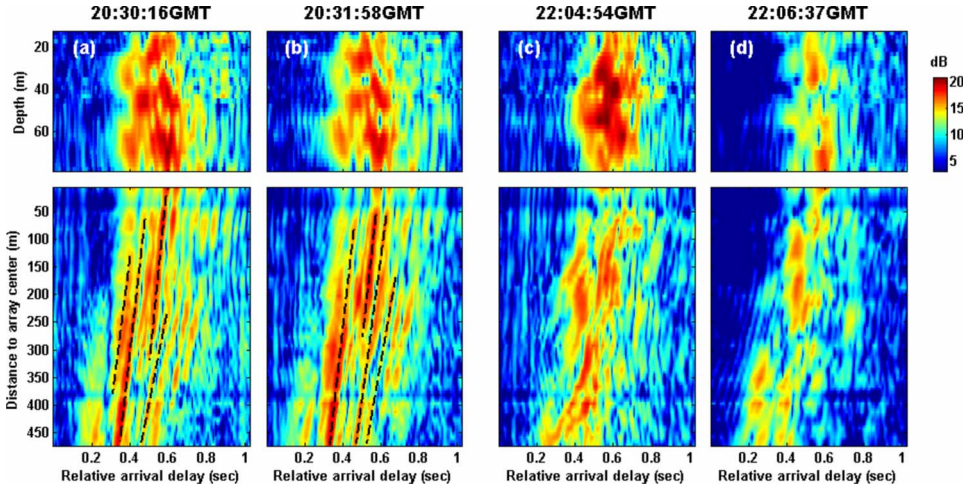

Fig. 3. (Color online) Received acoustic intensity on the Shark VHLA during two geotimes within the T_{g1} and T_{g2} periods. Upper panel shows the acoustic field on the VLA portion of the array while the lower panel shows the HLA portion. (a) T_g=20:30:16 GMT, (b) T_g=20:31:58 GMT, (c) T_g=22:04:54 GMT, (d) T_g=22:06:37 GMT.

ing signal energy during T_{g_1}. During T_{g_2} the same data format is shown. At 22:04:54 GMT shown in Fig. 3(c), both the VLA and HLA show a drastic change in the arrival. The signal intensity becomes very strong; however, different arrivals are mixed together and difficult to separate. The parallel lines on the HLA were notably distorted. At 22:06:37 GMT shown in Fig. 3(d), the arrivals show a lack of structure as well as lower intensity. During the time period of T_{g_2} the ISW is occupying a large fraction of the acoustic track. Mm. 2 shows a movie of the acoustic signal arrival on the Shark VHLA during the two periods T_{g_1} and T_{g_2}. To further quantify these results, we next calculate the average intensity in geotime and depth for the periods, T_{g_1} and T_{g_2}.

Mm. 2. Movie of the acoustic signal arrival on the Shark VHLA during the two periods T_{g_1} and T_{g_2}. This is a file of type gif (14 MB).

3. Intensity variations

Based on the theory proposed in our previous work,[3] the angle between the ISW fronts and the acoustic track determines the mechanism of the intensity fluctuations. Small angles provide horizontal refraction and focusing while larger angles cause mode coupling. Between these limits, there is an angular region for which the propagation is adiabatic. During internal wave Event 50, the ISW fronts passed through the acoustic track at an angle of about 5° providing the condition for horizontal refraction. Prior to the ISW arrival, we observe stable adiabatic propagation in a stable water column. Hence, a transition can indeed be observed between these two mechanisms.

To show a focusing event, we consider two geotimes: (a) T_{g_1} when the leading internal wave front had not reached the acoustic track and, (b) T_{g_2} when the internal wave packet occupied most of the acoustic track. We calculate the total intensity integrated over the depth H as

$$I(T) = \int_0^H I(z,T)dz, \tag{1}$$

where $I(z,T)=(1/\rho c)\int_{\tau}^{\tau+\Delta\tau} p^2(z,T,t)dt$ is the intensity of the signal arrivals integrated over a pulse length $\Delta\tau$ at a given depth z, where p is acoustic pressure, ρ is water density, and c is sound speed. The distribution of the ISWs in the horizontal plane can be assessed by carefully examining the radar image and the depth distribution of the temperature at three points (SW45, SW20, SW54) along the acoustic track.

The temperature distribution starting at 20:30:00 GMT (T_{g_1}) for the transmission period (i.e., ~7.5 min) at three different moorings shows very little fluctuation along the acoustic track (see Fig. 2). This indicates that the ISW has not reached the acoustic track during T_{g_1}, as is also shown in the radar image. In Fig. 4(a) we show a plot of $I(z,T)$ for the VLA. It is shown that for a repeated pulse of the same radiated intensity, only minor temporal intensity variation exists. In Fig. 4(b) we plot the depth integrated intensity for all geotimes, $I(T)$. The very small fluctuations (~3 dB) at T_{g_1} indicate a quiescent condition without ISWs in the track. This means that during this period of observation there is no redistribution of sound energy in the horizontal plane, i.e., there is no horizontal refraction. Small variations of the depth distribution of the sound intensity correspond to the adiabatic case. Figure 4(c) shows the acoustic intensity on the HLA. There are no apparent temporal intensity variations on the HLA during this geotime.

$I(z,T)$ for T_{g_2} is plotted in Fig. 4(d). Here we see increasing and decreasing trends in sound intensity over the VLA, which are synchronous in depth. The average intensity $I(T)$ using Eq. (1) peaks to ~35 dB around 22:04:30–22:05:00 GMT, and decreases to ~20 dB around 22:06:37 GMT as shown in Fig. 4(e). This significant fluctuation corresponds to redistribution of the acoustic energy in the horizontal plane, which in the limit can be referred to as focusing or defocusing events and is related to the position of the source and/or receiver with respect to

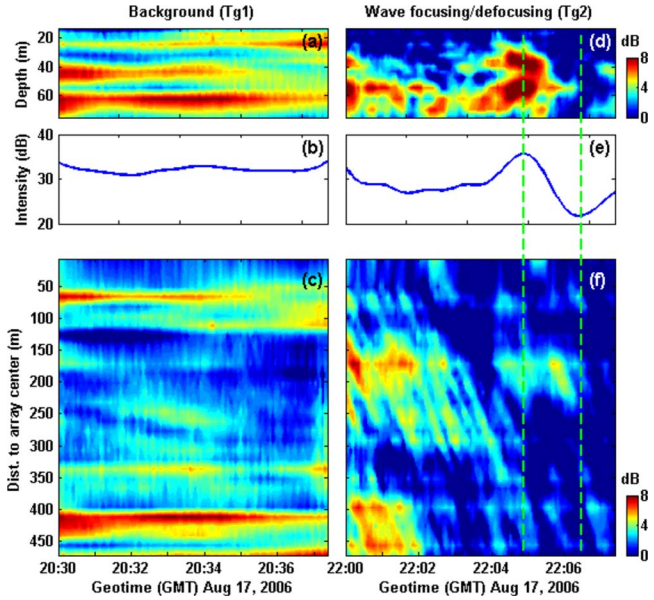

Fig. 4. (Color online) Received acoustic intensity during a 440 s (~7.33 min) transmission period for two geotimes, T_{g1} (from 20:30:00 to 20:37:20 GMT): (a) Depth distribution of total intensity per pulse $I(z,T)$, (b) depth integrated intensity, $I(T)$ for VLA, (c) total intensity $I(x,T)$ for HLA; and T_{g2} (22:00:00–22:07:20 GMT): (d) depth distribution of total intensity per pulse $I(z,T)$, (e) depth integrated intensity, $I(T)$ for VLA, (f) total intensity $I(x,T)$ for HLA.

the internal wave crests. The focusing and defocusing are also shown in Figs. 3(c) and 3(d). In this case (i.e., T_{g_2}), the receiver is between two adjacent maxima of the thermocline displacement, and the high intensity fluctuations (~15 dB peak to peak) are due to horizontal refraction effects similar to those shown in previous studies.[3] Temporal fluctuations correlate with oscillations of the thermocline layer at the receiver (see Fig. 2) due to ISWs (period is ~7–8 min). The fluctuations in the presence of internal waves (i.e., at T_{g_2}) are about 15 dB, which are much larger than those of T_{g_1} (~3 dB) with no internal wave in the acoustic track. Although the total jump in the thermocline thickness (i.e., from ~15 m to ~30 m) could make a difference in the "absolute" value of the acoustic intensity, it does not play a significant role in the temporal intensity fluctuation with periods corresponding to the ISW.

As in the quiescent case shown above, Fig. 4(f) shows the acoustic intensity on the HLA for the active period (T_{g_2}). During the geotime of about 7.33 min, we see the variation of the sound field at the horizontal array. For the variation observed during the first 3 min, there are two large intensity maxima observed at the HLA. These become weaker and disappear during the second half of the time period (after 22:03 GMT). This behavior, in our opinion, is a manifestation of horizontal redistribution of the sound intensity, which we call focusing/defocusing phenomena. The sloped intensity modulations correspond to the motion of an interference pattern registered on the horizontal array, which can be a result from any motion of the water layer (such as an ISW packet). The velocity of this interference pattern is estimated as 1–1.5 m/s from the acoustic data [shown as a slope in Fig. 4(f)]. This may not be directly related to the velocity of the internal solitons (measured from shipboard radar to be about 1 m/s). Further detailed modeling is needed to understand the nature of these fluctuations and their relationship to the slope of the lines shown in Fig. 4(f).

4. Summary

The SW06 experiment has provided high quality acoustic and environmental data to investigate the acoustic wave interaction with internal waves. Preliminary analysis of the acoustic data and

observations of radar images and temperature records shows that during the passage of an ISW event, horizontal refraction results in significant acoustic intensity variation. This observation agrees with the recently proposed theory of sound propagation through ISW.[3] Future work includes mode and frequency filtering of this acoustic data as well as modeling to establish the transition of acoustic field behavior from adiabatic to other mechanisms when an ISW passes an acoustic track.

Acknowledgments

The authors wish to thank all participants of the SW06 experiment, especially the scientific and ship personnel aboard the R/V SHARP and R/V OCEANUS. This research was supported by the Ocean Acoustic Program (321OA) of the Office of Naval Research through Grant No. N00014-07-1-0546.

References and links

[1]M. Badiey, Y. Mu, J. Lynch, J. R. Apel, and S. Wolf, "Temporal and azimuthal dependence of sound propagation in shallow water with internal waves," IEEE J. Ocean. Eng. **27**(1), 117–129 (2002).

[2]M. Badiey, B. G. Katsnelson, J. F. Lynch, S. Pereselkov, and W. L. Siegmann, "Measurement and modeling of three-dimensional sound intensity variations due to shallow-water internal waves," J. Acoust. Soc. Am. **117**(2), 613–625 (2005).

[3]M. Badiey, B. G. Katsnelson, J. F. Lynch, and S. Pereselkov, "Frequency dependence and intensity fluctuations due to shallow water internal waves," J. Acoust. Soc. Am. **122**(2), 747–760 (2007).

[4]A. E. Newhall, T. F. Duda, J. D. I. K. von der Heydt, J. N. Kemp, S. A. Lerner, S. P. Liberatore, Y.-T. Lin, J. F. Lynch, A. R. Maffei, A. K. Morozov, A. Shmelev, C. J. Sellers, and W. E. Witzell, "Acoustic and oceanographic observations and configuration information for the WHOI moorings for the SW06 experiment," WHOI technical report No. WHOI-2007-04, (2007).

[5]J. M. Collis, T. F. Duda, J. F. Lynch, and H. A. DeFerrari, "Observed limiting cases of horizontal field coherence and array performance in a time-varying internal wavefield," J. Acoust. Soc. Am. **124**(3), EL97–EL103 (2008).